

Modeling and fast output sampling feedback control of a smart Timoshenko cantilever beam

T. C. Manjunath[†]

Interdisciplinary Programme in Systems and Control Engineering, Indian Institute of Technology Bombay, 101B, ACRE Building, Mumbai-400076, Maharashtra, India

B. Bandyopadhyay[‡]

Systems and Control Engineering, I.I.T. Bombay, Powai, Mumbai-76, India

(Received December 1, 2004, Accepted April 26, 2005)

Abstract. This paper features about the modeling and design of a fast output sampling feedback controller for a smart Timoshenko beam system for a SISO case by considering the first 3 vibratory modes. The beam structure is modeled in state space form using FEM technique and the Timoshenko beam theory by dividing the beam into 4 finite elements and placing the piezoelectric sensor/actuator at one location as a collocated pair, i.e., as surface mounted sensor/actuator, say, at FE position 2. State space models are developed for various aspect ratios by considering the shear effects and the axial displacements. The effects of changing the aspect ratio on the master structure is observed and the performance of the designed FOS controller on the beam system is evaluated for vibration control.

Keywords: smart structure; Timoshenko beam; fast output sampling feedback control; finite element method; state space model; vibration control; aspect ratio; LMI.

1. Introduction

Piezoelectric materials are capable of altering the structure's response through sensing, actuation and control. Piezoelectric elements can be incorporated into a laminated composite structure, either by embedding it or by mounting it onto the surface of the host structure (Culshaw 1992). Vibration control of any system is always a formidable challenge for any system designer. Active control of vibrations relieves a designer from strengthening the structure from dynamic forces and the structure itself from extra weight and cost. The need for intelligent structures such as smart structures arises from the high performance requirements of such structural members in numerous applications. Intelligent structures are those which incorporate actuators and sensors that are highly integrated into the structure and have structural functionality, as well as highly integrated control logic, signal conditioning and power amplification electronics (Crawley and Luis 1987).

[†]IEEE/SPIE/IOP Student member, Assistant Professor, Dept. of Electronics Eng. since September 1996, Fr. Conceicao Rodrigues College of Eng., Bandra (West), Mumbai - 400050, Maharashtra, India, E-mail: tmanju@sc.iitb.ac.in
[‡]Professor and Convener, E-mail: bijnan@ee.iitb.ac.in

A vibration control system consists of 4 parts, viz., actuator, controller, sensor and the system or the plant, which is to be controlled. When an external force f_{ext} is applied to the beam, it is subjected to vibrations. These vibrations should be suppressed. Fully active actuators like the Piezoelectrics, MR Fluids, Piezoceramics, ER Fluids, Shape Memory Alloys, PVDF, etc., can be used to generate a secondary vibrational response in a mechanical system. This could reduce the overall response of the system plant by the destructive interference with the original response of the system, caused by the primary source of vibration (Baily and Hubbard 1985, Hanagud, *et al.* 1992, Crawley 1987, Fanson 1990).

Extensive research in modeling of piezoelectric materials in building actuators and sensors for structure is reported. Investigations of Crawley and Luis (1987) emphasized on the derivation of sensor/actuator modeling of piezo-electric materials. Moreover, the control analysis of cantilever beams using these sensors/actuators have been studied by Bailey and Hubbard (1985). Culshaw (1992) gave a brief introduction to the concept of smart structure, its benefits and applications. Hanagud, *et al.* (1992) developed a Finite Element Model (FEM) for an active beam with many distributed piezoceramic sensors/actuators coupled by signal conditioning systems and applied optimal output feedback control. Fanson, *et al.* (1990) performed some experiments on a beam with piezoelectrics using positive position feedback. Hwang and Park (1993) presented a FE model for piezoelectric sensors and actuators. Choi, *et al.* (1995) discussed about the control techniques of flexible structures using distributed piezoelectric sensors/actuators. Feedback control of vibrations in mechanical systems has numerous applications, like in aircrafts, active noise and shape control, acoustic control, control of antennas, control of space structures and in the control of flexible manipulators. A precise mathematical model is required for the controller design for vibration control to predict the structure's response. Two different models are normally used, viz., Euler-Bernoulli and the Timoshenko model.

In *Euler-Bernoulli beam theory*, the assumption made is, before and after bending the plane cross section of the beam remains plane and normal to the neutral axis. This assumption is valid if length to thickness ratio is large and for small deflection of beam. However, if length to thickness ratio is small, plane section will not remain normal to the neutral axis after bending. In practical situations, a large number of modes of vibrations contribute to the structure's performance. Since the shear forces, axial displacement are neglected in *Euler-Bernoulli theory*, slightly inaccurate results are obtained. *Timoshenko Beam Theory* is used to overcome the drawbacks of the Euler-Bernoulli beam theory.

In *Timoshenko beam theory*, cross sections remains plane and rotate about the same neutral axis as the Euler-Bernoulli model, but do not remain normal to the deformed longitudinal axis. The deviation from normality is produced by a transverse shear that is assumed to be constant over the cross section. Thus, the Timoshenko Beam model is superior to Euler-Bernoulli model in precisely predicting the beam response. Timoshenko beam theory is used in the present work to generate the FE model of a cantilever beam with surface mounted sensor and actuator as a collocated pair, i.e., one above and below the corresponding finite element of the beam. Further, the fast output sampling feedback control design and its application to control the structural vibration modes of a smart cantilever beam is considered.

The outline of the paper is as follows. A brief review of related literature about the types of beam models and embedded shear actuation is given in Section 2. Section 3 gives a brief introduction to the modeling technique (sensor/actuator model, finite element model, state space model) of the smart cantilever beam. Justification for the use of Timoshenko beam in the research work is presented in Section 4. A brief review of the controlling technique, viz., the fast output sampling feedback control technique to control the first three modes of vibration of the system for different aspect ratios of the beam is discussed in Section 5. The simulation results and discussions are presented in Section 6. Conclusions are drawn in Section 7.

2. Review of beam models and embedded shear piezo actuation

The study of physical systems such as beams frequently results in partial differential equations, which either cannot be solved analytically, or lack an exact analytic solution due to the complexity of the boundary conditions. For a realistic and detailed study, a numerical method must be used to solve the problem. The finite element method is often found the most adequate. Over the years, with the development of modern computers, the finite element method has become one of the most important analysis tools in engineering. Basically, the finite element method consists of a piecewise application of classical variational methods to smaller and simpler sub domains called finite elements connected to each other in a finite number of points called nodes. Two beam models in common use in the structural mechanics are the Euler-Bernoulli beam model and the Timoshenko beam model, which are considered here below.

2.1. Euler-Bernoulli model

This model often called as the classical beam model accounts for the bending moment effects on stresses and deformations. The effect of transverse shear forces on beam deformation is neglected. Its fundamental assumption is that cross sections remain plane and normal to the deformed longitudinal axis before and after bending as shown in Fig. 1. Here, the total rotation θ is due to bending stress alone neglecting transverse shear stress. This rotation occurs about a neutral axis that passes through the centroid of the cross section of the beam as shown in Fig. 1. Crawley, *et al.* (1987) have developed analytical models of beams with piezoelectric actuators. These models illustrate the mechanics of Euler-Bernoulli beams with surface mounted actuators and the analytical results have been verified by carrying out experiments.

2.2. Timoshenko model

This model corrects the classical beam model with first-order shear deformation effects. In this model, the cross sections of the beam remain plane and rotate about the neutral axis, but do not remain

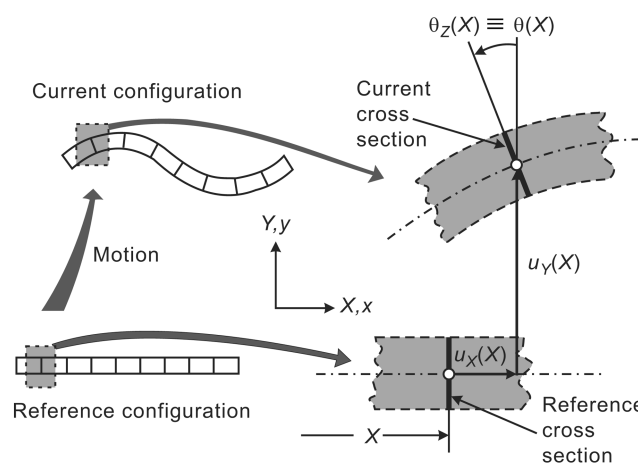


Fig. 1 Euler-Bernoulli beam model

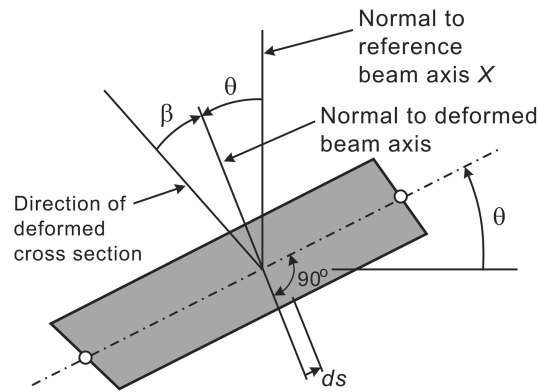


Fig. 2 Timoshenko beam model

normal to the deformed longitudinal axis as shown in Fig. 2. The total slope of the beam in this model consists of two parts, one due to bending θ , and the other due to shear β . Chandrashekhara and Varadarajan (1997) have presented a finite element model of a composite beam using a higher-order shear deformation theory. Piezoelectric elements have been used to produce a desired deflection in beams with Clamped-Free (C-F), Clamped-Clamped (C-C) and simply supported beams. Aldraihem, *et al.* (1997) have developed a laminated beam model using two theories; namely, Euler-Bernoulli beam theory and Timoshenko beam theory. Here, the piezoelectric layers have been used to control the vibration in a cantilever beam. Abramovich (1998) and Azulay, *et al.* (2004) has presented analytical formulation and closed form solutions of composite beams with piezoelectric actuators. Donthireddy and Chandrashekhara (1996) presented a new technique of modeling and shape control of composite beam with embedded piezoelectric actuators. A finite element model was designed for the dynamic analysis of Timoshenko beam by Thomas and Abbas (1975). Doschner and Enzmamam (1998) presented a new type of controller for the vibrations of the Timoshenko beam.

2.3. Shear piezoelectric actuation

Recently, shear piezoelectric actuators have been used to generate deflection and to reject vibration in beams. The idea of exploiting the shear mode to create transverse deflection in beams was first suggested by Sun and Zhang (1995). A finite element approach was used by Benjeddou, *et al.* (1999) to model a beam with shear and extension piezoelectric elements. The finite element model employed the displacement field of Zhang and Sun (1996). It was shown that the finite element results agree quite well with the analytical results. Raja, *et al.* (2002) extended the finite element model of Benjeddou's research team to include a vibration control scheme. It was observed that the shear actuator is more efficient in rejecting vibration than without considering the shear for the same control effort. Aldraihem and Khdeir (2000) proposed analytical models and exact solutions for beams with shear piezoelectric actuators. The models are based on Timoshenko beam theory and Higher-Order Beam Theory (HOBT). Exact solutions were obtained by using the state-space approach. The deflections of beams with various boundary conditions were investigated. The effect of shear coefficient was discussed in the Timoshenko beam theory by Cooper (1996). Deflection analysis of the beam with extension and shear piezoelectric patches was reported by Ahmed and Osama (2001). An improved two-node Timoshenko beam model was presented by Friedman and Kosmatka (1993).

3. Mathematical modeling of smart beam with surface mounted sensors and actuators

Numerous researchers have well established a mathematical finite element E-B model (Umapathy, *et. al.* 2000). These models do not consider the shear effects. Modeling of smart structures by shear deformable (Timoshenko) theory is limited. Shear effects in the control of a laminated beam become important when a high degree of accuracy is crucial and for beams with length to thickness (aspect) ratio less than 10. Thus, a shear deformable model will become essential when a high degree of accuracy is required for providing reliable results.

Consider a cantilever beam as shown in Fig. 3 divided into 4 finite elements. The piezoelectric element is bonded on a discrete section (at one finite element position, say at position 2) of the surface of the beam. The mass and stiffness of the adhesive used to bond the sensor/actuator pair to the master structure is being neglected. The smart cantilever beam model is developed using a piezoelectric beam element, which includes sensor and actuator dynamics and remaining beam elements as regular beam elements based on Timoshenko beam theory assumptions. The dimensions and properties of the steel cantilever beam and piezoelectric sensor/actuator used are given in Tables 1 and 2 respectively.

3.1. Finite element modeling of the regular beam element

A regular beam element is shown in Fig. 3. The longitudinal axis of the regular beam element lies along the X-axis. The element has constant moment of inertia, modulus of elasticity, mass density and length. The element is assumed to have two degrees of freedom w, θ . A bending moment and a transverse shear force acts at each nodal point (Friedman and Kosmatka 1993).

The displacement relation in the X, Y, and Z directions of the beam can be written as

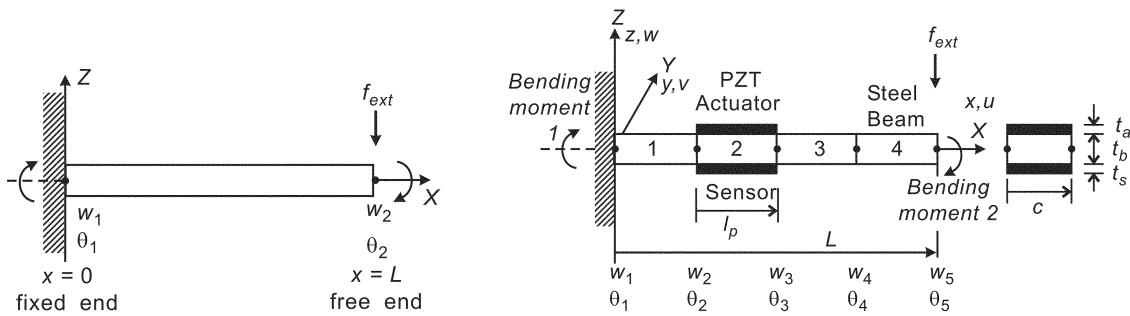


Fig. 3 A regular beam and a smart Timoshenko cantilever beam divided into 4 finite elements (piezo-patch placed at position 2) and a regular beam

Table 1 Physical parameters of the beam

Parameter	Symbol	Values
Total length of beam	l	0.5 m
Width	b	0.024 m
Young's modulus	E_b	193.096 Gpa
Density	ρ_b	8030 Kg/m ³
Constants used in C^*	α, β	0.001, 0.0001

Table 2 Properties of piezoelectric sensor / actuator

Parameter	Symbol	Values
length of PE	l_p	0.125 m
Width	b	0.024 m
Thickness	t_a	0.5 mm
Young's modulus	E_b	68 Gpa
Density	ρ_b	7700 Kg / m ³
Piezoelectric strain constant	d_{31}	125×10^{-12} mV ⁻¹
Piezoelectric stress constant	g_{31}	10.5×10^{-13} VmN ⁻¹

$$u(x, y, z, t) = z\theta(x, t) = z\left(\frac{\partial w}{\partial x} - \beta(x)\right), \quad v(x, y, z, t) = 0, \quad w(x, y, z, t) = w(x, t) \quad (1)$$

where w is the time dependent transverse displacement of the centroidal axis (along z axis), θ is the time dependent rotation of the cross-section about ' Y ' axis, u is the axial displacement along the x axis, v is the lateral displacement along the y axis which is equal to zero. The total slope of the beam consists of two parts, one due to bending, which is $\theta(x)$ and the other due to shear, which is $\beta(x)$ as shown in Fig. 2. The axial displacement of a point at a distance z from the centre line is only due to the bending slope and the shear slope has no contribution to this. The strain components of the beam are given as

$$\varepsilon_{xx} = \frac{\partial u}{\partial x} = \frac{\partial u}{\partial \theta} \frac{\partial \theta}{\partial x} = z \frac{\partial \theta}{\partial x}, \quad \varepsilon_{yy} = \frac{\partial v}{\partial y} = 0, \quad \varepsilon_{zz} = \frac{\partial w}{\partial z} = 0 \quad (2)$$

where ε_{xx} , ε_{yy} , ε_{zz} are the longitudinal strains or the tensile strains in the 3 directions, viz., in the x , y , z directions.

The shear strains γ induced in the beam along the 3 directions (viz., along x , y , z directions) are given by

$$\gamma_{xz} = \frac{1}{2} \left[\frac{\partial u}{\partial z} + \frac{\partial w}{\partial x} \right] = \frac{1}{2} \left[\theta + \frac{\partial w}{\partial x} \right] \quad (3)$$

$$\gamma_{yz} = \frac{1}{2} \left[\frac{\partial v}{\partial z} + \frac{\partial w}{\partial y} \right] = 0 \quad (4)$$

$$\gamma_{xy} = \frac{1}{2} \left[\frac{\partial u}{\partial y} + \frac{\partial v}{\partial x} \right] = 0 \quad (5)$$

The effect of shear strains along y and z directions is equal to zero. Thus, the stresses in the beam element are given as

$$\sigma_{xx} = E \varepsilon_{xx} = Ez \frac{\partial \theta}{\partial x} \quad (6)$$

$$\sigma_{xz} = G \gamma_{xz} = \frac{1}{2} G \left[\frac{\partial w}{\partial x} + \theta \right] = K \left[\frac{\partial w}{\partial x} + \theta \right] \quad (7)$$

where E is the Young's modulus of the beam material, G is shear modulus (or modulus of rigidity) of the beam material, σ_{xz} is the shear stress, σ_{xx} is the tensile stress and $K=G/2$ is the shear coefficient

which depends on the material definition and on the cross sectional geometry, usually taken equal to 5/6. The strain energy of the beam element depends upon the linear strain ε , the shear strain γ . The total strain energy of the beam is finally written as

$$U = \frac{1}{2} \int_0^L \begin{bmatrix} \frac{\partial \theta}{\partial x} \\ \frac{\partial w}{\partial x} + \theta \end{bmatrix}^T \begin{bmatrix} EI & 0 \\ 0 & KGA \end{bmatrix} \begin{bmatrix} \frac{\partial \theta}{\partial x} \\ \frac{\partial w}{\partial x} + \theta \end{bmatrix} dx \tag{8}$$

where I is the mass moment of inertia of the beam element, A is the area of cross section of the beam element and L is the length of the beam.

The kinetic energy T of the beam element depends on the sum of the kinetic energy due to the linear velocity \dot{w} and due to the angular twist $\dot{\theta}$. The total kinetic energy is finally written as

$$T = \frac{1}{2} \int_0^L \begin{bmatrix} \frac{\partial w}{\partial x} \\ \frac{\partial \theta}{\partial t} \end{bmatrix}^T \begin{bmatrix} \rho A & 0 \\ 0 & \rho I \end{bmatrix} \begin{bmatrix} \frac{\partial w}{\partial t} \\ \frac{\partial \theta}{\partial t} \end{bmatrix} dx \tag{9}$$

where ρ is the mass density of the beam material.

The total work done due to the external forces in the system is given by

$$W_e = \int_0^L \begin{bmatrix} w \\ \theta \end{bmatrix}^T \begin{bmatrix} q_d \\ m \end{bmatrix} dx \tag{10}$$

where q_d represents distributed force along the length of the beam and m represents the moment along the length of the beam.

The equation of motion is derived using Hamilton's principle which states as the total strain energy is equal to the sum of the change in the kinetic energy + the work done due to the external forces and is given by

$$\delta \Pi = \int_{t_1}^{t_2} (\delta U - \delta T - \delta W_e) dt = 0 \tag{11}$$

Here, δU , δT and δW_e are the variations of the strain energy, the kinetic energy, work done due to the external forces and T is kinetic energy, U is strain energy, W is the external work done, L is the length of the beam element and t is the time. Substituting the values of strain energy from Eq. (8), kinetic energy from Eq. (9) and external work done from Eq. (10) in Eq. (11) and integrating by parts, we get the governing equation of motion of a general shaped beam modeled with Timoshenko beam theory as

$$\frac{\partial \left\{ KGA \left(\frac{\partial w}{\partial x} + \theta \right) \right\}}{\partial x} + q_d = \rho A \frac{\partial^2 w}{\partial t^2} \tag{12}$$

$$\frac{\partial \left\{ EI \frac{\partial \theta}{\partial x} \right\}}{\partial x} - KGA \left(\frac{\partial w}{\partial x} + \theta \right) + M = \rho I \frac{\partial^2 \theta}{\partial t^2} \quad (13)$$

The R.H.S. of the Eq. (12) is the force, which is equal to mass multiplied by the linear acceleration, i.e., $F = ma$. The R.H.S. of the Eq. (13) is the moment which is equal to mass moment of inertia multiplied by the angular acceleration, i.e., mass moment of inertia $= I\alpha$. For the static case with no external force acting on the beam, the governing equation of motion reduces to

$$\frac{\partial \left\{ KGA \left(\frac{\partial w}{\partial x} + \theta \right) \right\}}{\partial x} = 0 \quad (14)$$

and

$$\frac{\partial \left\{ EI \frac{\partial \theta}{\partial x} \right\}}{\partial x} - KGA \left(\frac{\partial w}{\partial x} + \theta \right) = 0 \quad (15)$$

From Eqs. (14) and (15), it can be seen that this governing equation of the beam based on Timoshenko beam theory can only be satisfied if the polynomial order for w is selected one order higher than the polynomial order for θ . Let w be approximated by a cubic polynomial and θ be approximated by a quadratic polynomial as

$$w = a_1 + a_2x + a_3x^2 + a_4x^4 \quad (16)$$

$$\theta = b_1 + b_2x + b_3x^2 \quad (17)$$

Here, in Eqs. (16) and (17), x is the distance of the finite element node from the fixed end, a_i and b_j ($i = 1,2,3,4$) and ($j = 1,2,3$) are the unknown coefficients and are found out using the boundary conditions at the beam ends $x = (0, L)$ as

$$\text{at } x = 0, \quad w = w_1, \quad \theta = -\theta_1 \quad \text{and at } x = L, \quad w = w_2, \quad \theta = -\theta_2 \quad (18)$$

After applying boundary conditions from Eq. (18) on Eqs. (16) and (17), the unknown coefficients a_i and b_j can be resolved. Substituting the unknown coefficients a_i and b_j in Eqs. (16) and (17) and writing them in matrix form, we get, the transverse displacement, the first spatial derivative of the transverse displacement, the second spatial derivative of the transverse displacement and the time derivative of Eq. (16) as

$$[w(x, t)] = [N_w][q] \quad (19)$$

$$[w'(x, t)] = [N_\theta][q] \quad (20)$$

$$[w''(x, t)] = [N_\alpha][q] \quad (21)$$

$$[\dot{w}(x, t)] = [N_w][\dot{q}] \quad (22)$$

where q is the vector of displacements and slopes, $[\dot{q}]$ is the strain rate, $[N_w]^T$, $[N_\theta]^T$, $[N_a]^T$ are the mode shape functions (for displacement, rotations and accelerations) taking ϕ into consideration and are given in the appendix. The mass matrix of the particular regular beam element (also called as the local mass matrix) is the sum of the translational mass and the rotational mass and is given in matrix form as

$$[M^b] = \int_0^L \begin{bmatrix} [N_w] \\ [N_\theta] \end{bmatrix}^T \begin{bmatrix} \rho A & 0 \\ 0 & \rho I_{yy} \end{bmatrix} \begin{bmatrix} [N_w] \\ [N_\theta] \end{bmatrix} dx \tag{23}$$

Substituting the mode shape functions $[N_w]$, $[N_\theta]$ into Eq. (23) and integrating, we get the mass matrix of that particular regular beam element as

$$[M^b] = [M_{\rho A}] + [M_{\rho I}] \tag{24}$$

where $[M_{\rho A}]$ and $[M_{\rho I}]$ in Eq. (24) is associated with the translational inertia and rotary inertia as given in the appendix. The stiffness matrix $[K^b]$ of the regular beam element (also called as the local stiffness matrix) is the sum of the bending stiffness and the shear stiffness and is written in matrix form as

$$[K^b] = \int_0^L \begin{bmatrix} \frac{\partial}{\partial x}[N_\theta] \\ [N_\theta] + \frac{\partial}{\partial t}[N_w] \end{bmatrix}^T \begin{bmatrix} EI & 0 \\ 0 & KGA \end{bmatrix} \begin{bmatrix} \frac{\partial}{\partial x}[N_\theta] \\ [N_\theta] + \frac{\partial}{\partial t}[N_w] \end{bmatrix} dx \tag{25}$$

Substituting the mode shape functions $[N_w]$, $[N_\theta]$ into Eq. (25) and integrating, we get the stiffness matrix of that particular regular beam element as $[K^b]$ which is given in the appendix. The consistent force array is given as

$$\{F\} = \int_0^L \begin{bmatrix} [N_w] \\ [N_\theta] \end{bmatrix}^T \begin{bmatrix} q \\ m \end{bmatrix} dx \tag{26}$$

3.2. Finite Element Modeling of the piezoelectric beam element

The regular beam elements with the piezoelectric patches are shown in Fig. 3. The piezoelectric element is obtained by bonding the regular beam element with a layer of two piezoelectric patches, one above and the other below at one finite element position as a collocated pair. The bottom layer acts as the sensor and the top layer acts as an actuator. The element is assumed to have two structural degrees of freedom at each nodal point, which are, transverse deflection w , and an angle of rotation or slope θ and an electrical degree of freedom, i.e., the sensor voltage. The effect of shear is negligible in the piezoelectric patches, since they are very thin and light. So the piezoelectric layers are modeled based on Euler-Bernoulli beam theory and the middle steel layer, i.e., the regular steel beam is modeled based on Timoshenko beam theory. The mass matrix of that particular piezoelectric element is given by (Manjunath and Bandyopadhyay 2004, Umamathy and Bandyopadhyay 2000).

$$[M^p] = \frac{\rho_p A_p l_p}{420} \begin{bmatrix} 156 & 22l_p & 54 & -13l_p \\ 22l_p & 4l_p & 13l_p & -3l_p \\ 54 & 13l_p & 156 & -22l_p \\ -13l_p & -3l_p^2 & -22l_p & 4l_p^2 \end{bmatrix} \quad (27)$$

where

- ρ_p is the mass density of piezoelectric beam element,
- A_p is the area of the piezoelectric patch = $2t_a c$, i.e., the area sensor as well as actuator,
- c being the width of the beam and
- l_p is the length of the piezoelectric patch.

Similarly, we obtain the stiffness matrix $[K^{piezo}]$ of that particular piezoelectric element is obtained as

$$[K^p] = \frac{E_p I_p}{l_p} \begin{bmatrix} \frac{12}{l_p^2} & \frac{6}{l_p} & \frac{12}{l_p^2} & \frac{6}{l_p} \\ \frac{6}{l_p} & 4 & -\frac{6}{l_p} & 2 \\ -\frac{12}{l_p^2} & -\frac{6}{l_p} & \frac{12}{l_p^2} & -\frac{6}{l_p} \\ \frac{6}{l_p} & 2 & -\frac{6}{l_p} & 4 \end{bmatrix} \quad (28)$$

where $[E_p]$ is the modulus of elasticity of piezoelectric material, $[I_p]$ is the moment of inertia of the piezoelectric layer with respect to the neutral axis of the beam and given by

$$[I_p] = \frac{1}{12} c t_a^3 + c t_a \left(\frac{t_a + t_b}{2} \right)^2 \quad (29)$$

where t_b is the thickness of the beam and t_a is the thickness of the actuator also equal to the thickness of the sensor.

3.3. Mass and stiffness of the beam element with piezoelectric patch

The mass and stiffness matrix for that particular piezoelectric beam element (regular beam element with piezoelectric patches placed at the top and bottom surfaces) as a collocated pair is given by

$$[\mathbf{M}] = [M_{\rho A}] + [M_{\rho I}] + [M^p] \quad (30)$$

and,

$$[\mathbf{K}] = [K^b] + [K^p] \quad (31)$$

3.4. Piezoelectric strain rate sensors and actuators

The linear piezoelectric coupling between the elastic field and the electric field of a PZT material is expressed by the direct and converse piezoelectric constitutive equations as

$$D = d\sigma + e^T E_f, \quad \varepsilon = s^E \sigma + dE_f \quad (32)$$

where σ is the stress, ε is the strain, E_f is the electric field, D is the dielectric displacement, e is the permittivity of the medium, s^E is the compliance of the medium, and d is the piezoelectric constant.

3.4.1. Sensor equation

The direct piezoelectric equation is used to calculate the output charge produced by the strain in the structure. The total charge $Q(t)$ developed on the sensor surface (due to the strain) is the spatial summation of all point charges developed on the sensor layer and the corresponding current generated is given by

$$i(t) = z e_{31} c \int_0^{l_p} N_a^T \dot{\mathbf{q}} dx \quad (33)$$

where $z = t_b/2 + t_a$, e_{31} is the piezoelectric stress / charge constant, $\dot{\mathbf{q}}$ is the time derivative of the modal coordinate vector and N_a^T is the second spatial derivative of the mode shape function of the beam. This current is converted into the open circuit sensor voltage V^s using a signal-conditioning device with gain G_c and applied to an actuator with the controller gain K_c . The sensor output voltage obtained is as

$$V^s = G_c e_{31} z c \int_0^{l_p} N_a^T \dot{\mathbf{q}} dx \quad (34)$$

or can be expressed as a scalar vector product

$$V^s(t) = \mathbf{p}^T \dot{\mathbf{q}} \quad (35)$$

where \mathbf{p}^T is a constant vector. The input voltage to the actuator is $V^a(t)$ and is given by

$$V^a(t) = K_c G_c e_{31} z c \int_0^{l_p} N_a^T \dot{\mathbf{q}} dx \quad (36)$$

The cable capacitance between sensor and signal-conditioning device has been considered negligible and the temperature effects have been neglected. Note that the sensor output is a function of the second spatial derivative of the mode shape.

3.4.2. Actuator equation

The actuator strain is derived from the converse piezoelectric equation. The strain developed by the electric field (E_f) on the actuator layer is given by

$$\varepsilon_A = d_{31} E_f = d_{31} \frac{V^a(t)}{t_a} \quad (37)$$

When the input to the actuator $V^a(t)$ is applied in the thickness direction, the stress is

$$\sigma_A = E_p d_{31} \frac{V^a(t)}{t_a} \quad (38)$$

The resultant moment M_A acting on the beam is determined by integrating the stress through the structure thickness

$$M_A = E_p d_{31} \bar{z} V^a(t) \quad (39)$$

where \bar{z} , is the distance between the neutral axis of the beam and the piezoelectric layer. The control force applied by the actuator is

$$\mathbf{f}_{ctrl} = E_p d_{31} c \bar{z} \int_{l_p} N_\theta dx V^a(t) \quad (40)$$

or can be expressed as a scalar product

$$\mathbf{f}_{ctrl} = \mathbf{h} V^a(t) \quad (41)$$

where $[N_\theta]^T$ is the first spatial derivative of mode shape function of the beam and \mathbf{h}^T is a constant vector. If an external force \mathbf{f}_{ext} acts on the beam, then, the total force vector becomes

$$\mathbf{f}^t = \mathbf{f}_{ext} + \mathbf{f}_{ctrl} \quad (42)$$

3.5. Dynamic equation of the smart structure

The dynamic equation of the smart structure is obtained by using both the regular and piezoelectric beam elements given in Eqs. (24)-(28). The mass and stiffness of the entire beam, which is divided into 4 finite elements is assembled using the FEM technique and the assembled matrices (global matrices), \mathbf{M} and \mathbf{K} are obtained, which also includes the sensor/actuator mass and stiffness. The equation of motion of the smart structure is finally given by

$$\mathbf{M}\ddot{\mathbf{q}} + \mathbf{K}\mathbf{q} = \mathbf{f}_{ext} + \mathbf{f}_{ctrl} = \mathbf{f}^t \quad (43)$$

where \mathbf{q} is the nodal variable vector.

The generalized coordinates are introduced into the Eq. (43) in order to reduce it further such that the resultant equation represents the dynamics of the desired number of modes of vibration. Let

$$\mathbf{q} = \mathbf{T} \mathbf{g} \quad (44)$$

be the transformation where \mathbf{T} is the modal matrix containing the eigenvectors representing the desired number of modes of vibration of the cantilever beam. This method is used to derive the uncoupled equations governing the motion of the free vibrations of the system in terms of principal coordinates by introducing a linear transformation between the generalized coordinates \mathbf{q} and the principal coordinates \mathbf{g} . The Eq. (43) after applying the transformation and further simplifying becomes

$$\mathbf{M}^* \ddot{\mathbf{g}} + \mathbf{K}^* \mathbf{g} = \mathbf{f}_{ext}^* + \mathbf{f}_{ctrl}^* \quad (45)$$

where the matrices \mathbf{M}^* , \mathbf{K}^* , \mathbf{f}_{ext}^* and \mathbf{f}_{ctrl}^* are the generalized mass matrix, the generalized stiffness matrix, the generalized external force vector and the generalized control force vector which are given by $\mathbf{M}^* = \mathbf{T}^T \mathbf{M} \mathbf{T}$, $\mathbf{K}^* = \mathbf{T}^T \mathbf{K} \mathbf{T}$, $\mathbf{f}_{ext}^* = \mathbf{T}^T \mathbf{f}_{ext}$ and $\mathbf{f}_{ctrl}^* = \mathbf{T}^T \mathbf{f}_{ctrl}$. The structural modal damping matrix \mathbf{C}^* is introduced into the Eq. (45) by

$$\mathbf{C}^* = \alpha \mathbf{M}^* + \beta \mathbf{K}^* \quad (46)$$

where α and β are structural constants. Finally, the dynamic equation of the smart structure is given by

$$\mathbf{M}^* \ddot{\mathbf{g}} + \mathbf{C}^* \dot{\mathbf{g}} + \mathbf{K}^* \mathbf{g} = \mathbf{f}_{ext}^* + \mathbf{f}_{ctrl}^* \quad (47)$$

where \mathbf{C}^* is the generalized damping matrix.

3.6. State space model of the smart beam

The governing equation in Eq. (47) is often written in state space form and is obtained as follows. Let the transformation used be $\mathbf{g} = \mathbf{x}$.

$$\text{i.e.,} \quad \mathbf{g} = \begin{bmatrix} g_1 \\ g_2 \\ g_3 \end{bmatrix} = \begin{bmatrix} x_1 \\ x_2 \\ x_3 \end{bmatrix} = \mathbf{x} \quad (48)$$

$$\therefore, \quad \dot{\mathbf{g}} = \dot{\mathbf{x}} = \begin{bmatrix} \dot{x}_1 \\ \dot{x}_2 \\ \dot{x}_3 \end{bmatrix} = \begin{bmatrix} x_4 \\ x_5 \\ x_6 \end{bmatrix} \quad \text{and} \quad \ddot{\mathbf{g}} = \ddot{\mathbf{x}} = \begin{bmatrix} \dot{x}_4 \\ \dot{x}_5 \\ \dot{x}_6 \end{bmatrix} \quad (49)$$

$$\text{Thus,} \quad \begin{aligned} \dot{x}_1 &= x_4 \\ \dot{x}_2 &= x_5 \\ \dot{x}_3 &= x_6 \end{aligned} \quad (50)$$

Using Eqs. (48) - (50) in Eq. (47) becomes

$$\mathbf{M}^* \begin{bmatrix} \dot{x}_4 \\ \dot{x}_5 \\ \dot{x}_6 \end{bmatrix} + \mathbf{C}^* \begin{bmatrix} x_4 \\ x_5 \\ x_6 \end{bmatrix} + \mathbf{K}^* \begin{bmatrix} x_1 \\ x_2 \\ x_3 \end{bmatrix} = \mathbf{f}_{ext}^* + \mathbf{f}_{ctrl}^* \quad (51)$$

which can be further simplified as

$$\begin{bmatrix} \dot{x}_4 \\ \dot{x}_5 \\ \dot{x}_6 \end{bmatrix} = -\mathbf{M}^{*-1} \mathbf{K}^* \begin{bmatrix} x_1 \\ x_2 \\ x_3 \end{bmatrix} - \mathbf{M}^{*-1} \mathbf{C}^* \begin{bmatrix} x_4 \\ x_5 \\ x_6 \end{bmatrix} + \mathbf{M}^{*-1} \mathbf{f}_{ext}^* + \mathbf{M}^{*-1} \mathbf{f}_{ctrl}^* \quad (52)$$

The generalized external force coefficient vector is

$$\mathbf{f}_{ext}^* = \mathbf{T}^T \mathbf{f}_{ext} = \mathbf{T}^T f r(t) \quad (53)$$

where $r(t)$ is the external force input to the beam.

The generalized control force coefficient vector is

$$\mathbf{f}_{ctrl}^* = \mathbf{T}^T f_{ctrl} = \mathbf{T}^T \mathbf{h} V^a(t) = \mathbf{T}^T \mathbf{h} u(t) \quad (54)$$

where the voltage $V^a(t)$ is the input voltage to the actuator from the controller and is nothing but the control input $u(t)$ to the actuator, \mathbf{h} is a constant vector which depends on the actuator type and its position on the beam.

So, using the Eqs. (53) and (54) in Eq. (52), the state space equation for the smart beam is represented as

$$\begin{bmatrix} \dot{x}_1 \\ \dot{x}_2 \\ \dot{x}_3 \\ \dot{x}_4 \\ \dot{x}_5 \\ \dot{x}_6 \end{bmatrix} = \begin{bmatrix} 0 & I \\ -\mathbf{M}^{*-1} \mathbf{K}^* & -\mathbf{M}^{*-1} \mathbf{C}^* \end{bmatrix} \begin{bmatrix} x_1 \\ x_2 \\ x_3 \\ x_4 \\ x_5 \\ x_6 \end{bmatrix} + \begin{bmatrix} 0 \\ \mathbf{M}^{*-1} \mathbf{T}^T \mathbf{h} \end{bmatrix} \mathbf{u}(t) + \begin{bmatrix} 0 \\ \mathbf{M}^{*-1} \mathbf{T}^T \mathbf{f} \end{bmatrix} r(t) \quad (55)$$

where $u(t)$ is the control input, $r(t)$ is the external input to the system and \mathbf{f} is the total force coefficient vector.

The sensor equation is modeled as

$$V^s(t) = \mathbf{p}^T \dot{\mathbf{q}} = y(t) \quad (56)$$

where \mathbf{p}^T is a constant vector which depends on the piezoelectric sensor characteristics and on the position of the sensor location on the beam. Thus, the sensor output equation for a SISO case is given by

$$y(t) = \mathbf{p}^T \dot{\mathbf{q}} = \mathbf{p}^T \mathbf{T} \dot{\mathbf{g}} = \mathbf{p}^T \mathbf{T} \begin{bmatrix} x_4 \\ x_5 \\ x_6 \end{bmatrix} \quad (57)$$

which can be written as

$$y(t) = \begin{bmatrix} 0 & \mathbf{p}^T & \mathbf{T} \end{bmatrix} \begin{bmatrix} x_1 \\ x_2 \\ x_3 \\ x_4 \\ x_5 \\ x_6 \end{bmatrix} \quad (58)$$

The state space model (state equation and the output equation) of the smart structure developed for the system in Eqs. (55) and (58) thus, is given by

$$\dot{\mathbf{x}} = \mathbf{A}\mathbf{x}(t) + \mathbf{B}u(t) + \mathbf{E}r(t), \quad y(t) = \mathbf{C}^T\mathbf{x}(t) + \mathbf{D}u(t) \quad (59)$$

with

$$\mathbf{A} = \begin{bmatrix} 0 & I \\ -\mathbf{M}^{*-1}\mathbf{K}^* & -\mathbf{M}^{*-1}\mathbf{C}^* \end{bmatrix}_{(6 \times 6)}; \quad \mathbf{B} = \begin{bmatrix} 0 \\ \mathbf{M}^{*-1}\mathbf{T}^T\mathbf{h} \end{bmatrix}_{(6 \times 1)}; \\ \mathbf{C} = \begin{bmatrix} 0 & \mathbf{p}^T & \mathbf{T} \end{bmatrix}_{(1 \times 6)}; \quad \mathbf{D} = \text{null matrix}; \quad \mathbf{E} = \begin{bmatrix} 0 \\ \mathbf{M}^{*-1}\mathbf{T}^T\mathbf{f} \end{bmatrix}_{(6 \times 1)} \quad (60)$$

4. Justification of the use of Timoshenko beam theory for the modeling of smart beam

The state space representation of the cantilever beam with surface mounted sensor / actuator in Eq. (59) is obtained by using 3 regular beam elements and 1 piezoelectric beam element placed at finite element position 2 as shown in Fig. 3. Different state space models of the system are obtained by

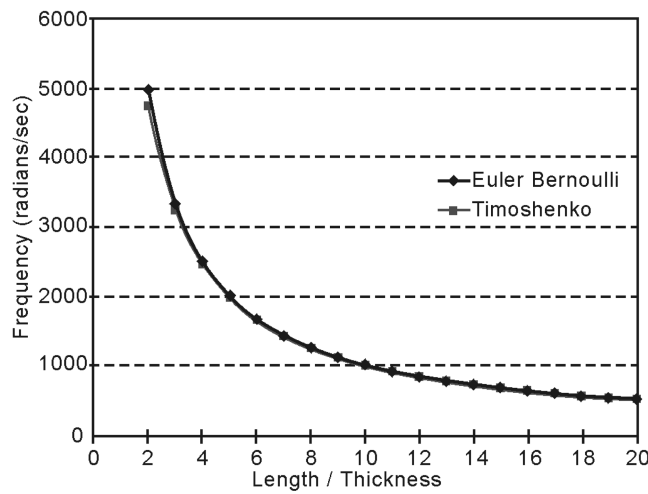


Fig. 4 Variation of first natural frequency with length/thickness ratio

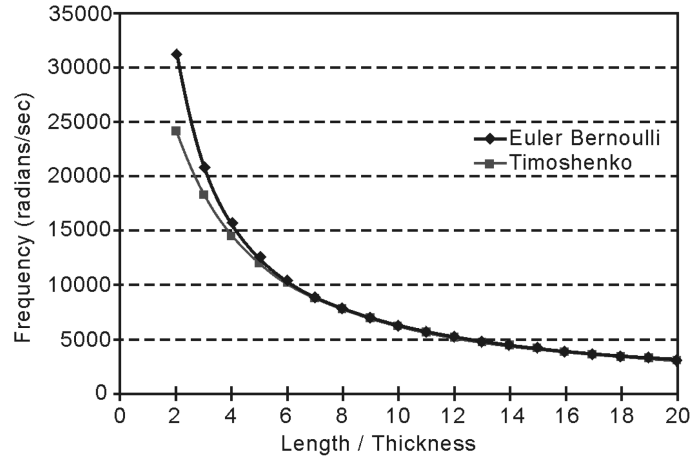


Fig. 5 Variation of second natural frequency with length/thickness ratio

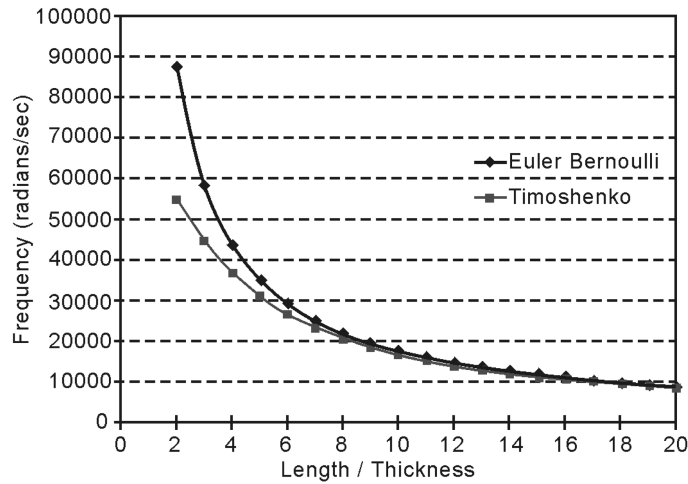


Fig. 6 Variation of third natural frequency with length/thickness ratio

varying the length to thickness ratio from 8 to 15. The length of the beam is kept constant at 50 cm and the thickness is varied to change the aspect ratio. The width of the beam is taken as 2.4 cm. The first and second natural frequencies of the 3 systems were calculated and compared with the corresponding natural frequencies obtained using the Euler-Bernoulli beam model.

Figs. 4 to 6 show the variation of the first and second natural frequencies of both Timoshenko and Euler-Bernoulli beam models with change in the length to thickness ratio. It is clear from Fig. 4 that the first natural frequency predicted by both the theories is almost the same. Since many modes contribute to a structure's response, it can be inferred from Figs. 5 and 6 that there is a large difference in the second and third natural frequencies predicted by Timoshenko and Euler-Bernoulli beam theories especially for small length to thickness ratios (aspect ratio < 10). Thus, the Timoshenko beam theory can predict the dynamic characteristics of the beam more accurately over the entire range of length by thickness ratio. Since Timoshenko beam model is closer to the actual model, it is used as the basis for controller design in our research work.

5. Fast output sampling feedback control technique

In the following section, we develop the control strategy for the SISO representation of the developed smart structure model using the fast output sampling feedback control law (Werner 1998, Werner and Furuta 1995) with 1 actuator input u and 1 sensor output y and varying the aspect ratios of the beam. In this type of control law as shown in Fig. 7, the value of the input at a particular moment depends on the output value at a time prior to this moment (namely at the beginning of the period). Werner and Furuta have shown that the poles of the discrete time control system could be assigned arbitrarily (within the natural restriction that they should be located symmetrically with respect to the real axis) using the fast output sampling technique. Since the feedback gains are piecewise constants, their method could easily be implemented, guarantees the closed loop stability and indicated a new possibility. Such a control law can stabilize a much larger class of systems.

Consider a plant described by a LTI state space model given by

$$\dot{x}(t) = Ax(t) + Bu(t), \quad y(t) = Cx(t) \tag{61}$$

where $x \in \mathfrak{R}^n$, $u \in \mathfrak{R}^m$, $y \in \mathfrak{R}^p$, $A \in \mathfrak{R}^{n \times n}$, $B \in \mathfrak{R}^{n \times m}$, $C \in \mathfrak{R}^{p \times n}$, A, B, C , are constant matrices of appropriate dimensions and it is assumed that the model is controllable and observable. Assume that output measurements are available at time instants $t = k\tau$, where $k = 0, 1, 2, 3, \dots$. Now, construct a discrete linear time invariant system from these output measurements at sampling rate $1/\tau$ (sampling interval of τ secs) during which the control signal u is held constant. The system obtained so is called as the τ system and is given by

$$x((k + 1)\tau) = \Phi_\tau x(k\tau) + \Gamma_\tau u(k\tau), \quad y(k\tau) = Cx(k\tau) \tag{62}$$

where $\Phi_\tau, \Gamma_\tau, C$ are constant matrices of appropriate dimensions. Assume that the plant is to be controlled by a digital computer, with sampling interval τ and zero order hold and that a sampled data state feedback design has been carried out to find a state feedback gain F such that the closed loop system

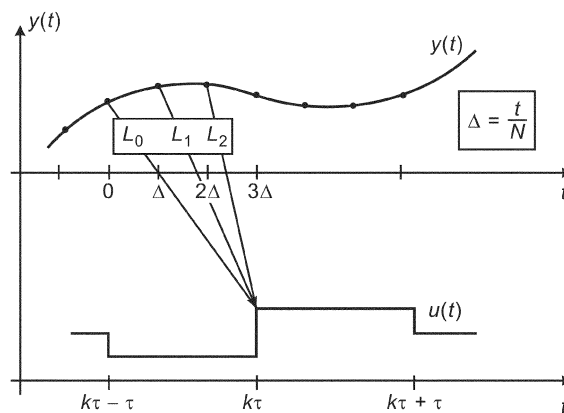


Fig. 7 Graphical illustration of fast output sampling feedback method

$$x(k\tau + \tau) = (\Phi_\tau + \Gamma_\tau F)x(k\tau) \quad (63)$$

has desirable properties.

Let $\Delta = \frac{\tau}{N}$, where $N >$ the observability index ν of the system. The control signal $u(k)$, which is applied during the interval $k\tau \leq t \leq (k+1)\tau$ is then generated according to

$$u(k) = \begin{bmatrix} L_0 & L_1 & \cdots & L_{N-1} \end{bmatrix} \begin{bmatrix} y(k\tau - \tau) \\ y(k\tau - \tau + \Delta) \\ \vdots \\ y(k\tau - \Delta) \end{bmatrix} = Ly_k \quad (64)$$

where the matrix blocks L_j represent the output feedback gains and the notation Ly_k has been introduced here for convenience. Note that $1/\tau$ is the rate at which the loop is closed, whereas the output samples are taken at the times N -times faster rate $1/\Delta$. To show how a FOS controller in Eq. (64) can be designed to realize the given sampled data state feedback gain for a controllable and observable system, we construct a fictitious, lifted system for which the Eq. (64) can be interpreted as static output feedback (Syrmos, *et al.* 1997, Werner, *et al.* 1995). Let (Φ, Γ, C) denote the system in Eq. (61) sampled at the rate $1/\Delta$. Consider the discrete time system having at time $t = k\tau$, the input $u_k = u(k\tau)$, the state $x_k = x(k\tau)$ and the output y_k as

$$x_{k+1} = \Phi_\tau x_k + \Gamma_\tau u_k, \quad y_{k+1} = \mathbf{C}_0 x_k + \mathbf{D}_0 u_k \quad (65)$$

where

$$\mathbf{C}_0 = \begin{bmatrix} C \\ C\Phi \\ \vdots \\ C\Phi^{N-1} \end{bmatrix}; \quad \mathbf{D}_0 = \begin{bmatrix} 0 \\ C\Gamma \\ \vdots \\ C \sum_{j=0}^{N-2} \Phi^j \Gamma \end{bmatrix} \quad (66)$$

Now, design a state feedback gain F such that $(\Phi_\tau + \Gamma_\tau F)$ has no Eigen values at the origin and provides the desired closed loop behavior. Then, assuming that in the interval $k\tau \leq t \leq (k\tau + \tau)$,

$$u(t) = Fx(k\tau) \quad (67)$$

one can define the fictitious measurement matrix,

$$\mathbf{C}(F, N) = (\mathbf{C}_0 + \mathbf{D}_0 F)(\Phi_\tau + \Gamma_\tau F)^{-1} \quad (68)$$

which satisfies the fictitious measurement equation

$$y_k = \mathbf{C}x_k \quad (69)$$

For L to realize the effect of F , it must satisfy the equation

$$\mathbf{LC} = F \quad (70)$$

Let ν denote the observability index of (Φ, Γ, C) . It can be shown that for $N \geq \nu$, generically \mathbf{C} has full column rank, so that any state feedback gain can be realized by a fast output sampling gain \mathbf{L} . If the initial state is unknown, there will be an error $\Delta u_k = u_k - Fx_k$ in constructing the control signal under the state feedback; one can verify that the closed-loop dynamics are governed by

$$\begin{bmatrix} x_{k+1} \\ \Delta u_{k+1} \end{bmatrix} = \begin{bmatrix} \Phi_\tau + \Gamma_\tau F & \Gamma_\tau \\ 0 & \mathbf{LD}_0 - F\Gamma_\tau \end{bmatrix} \begin{bmatrix} x_k \\ \Delta u_k \end{bmatrix} \quad (71)$$

The system in Eq. (65) is stable if F stabilizes and only if (Φ_τ, Γ_τ) and the matrix $(\mathbf{LD}_0 - F\Gamma_\tau)$ has all its Eigen values inside the unit circle. The problem with controllers obtained in this way is that, although they are stabilizing and achieve the desired closed loop behavior in the output sampling instants, they may cause an excessive oscillation between sampling instants. The fast output sampling feedback gains obtained may be very high. To reduce this effect, we relax the condition that L exactly satisfy the linear Eq. (70) and include a constraint on the gain L . Thus, we arrive at the following in Eq. (72) as

$$\|L\| < \rho_1; \quad \|\mathbf{LD}_0 - F\Gamma_\tau\| < \rho_2; \quad \|\mathbf{LC} - F\| < \rho_3 \quad (72)$$

This can be formulated in the form of Linear Matrix Inequalities as

$$\begin{bmatrix} -\rho_1^2 I & \mathbf{L} \\ \mathbf{L}^T & -I \end{bmatrix} < 0; \quad \begin{bmatrix} -\rho_2^2 I & \mathbf{LD}_0 - F\Gamma_\tau \\ (\mathbf{LD}_0 - F\Gamma_\tau)^T & -I \end{bmatrix} < 0; \quad \begin{bmatrix} -\rho_3^2 I & \mathbf{LC} - F \\ (\mathbf{LC} - F)^T & -I \end{bmatrix} < 0 \quad (73)$$

In this form, the LMI control optimization toolbox is used for the synthesis of L (Yong, Lam and Sun 1998).

6. Control simulations of the smart beam

The FEM and the state space model of the smart cantilever beam is developed in MATLAB using Timoshenko beam theory. A sixth order state space model of the system is obtained on retaining the first three modes of vibration of the system. Different state space models of the smart cantilever beam are obtained by varying the aspect ratio from 8 to 15. The length of the beam is kept constant and the thickness of the beam is varied. The fast output sampling feedback control technique discussed in previous section is used to design a controller to suppress the vibrations of the cantilever beam. Simulations are carried out in MATLAB.

The cantilever beam is divided into 4 finite elements and the sensor and actuator as a collocated pair are placed near by the fixed end as shown in Fig. 3. Three different cases of the beams having different aspect ratios are considered.

In the first case, the aspect ratio is taken equal to 15. The length of the beam element is 5 cm and its cross section is 3.33 mm by 2.4 cm. The length of the piezoelectric patch is 5 cm and its cross section is

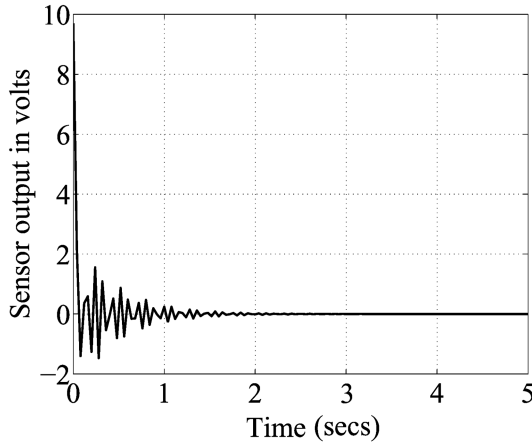


Fig. 8 Open loop response of smart cantilever beam with aspect ratio=15

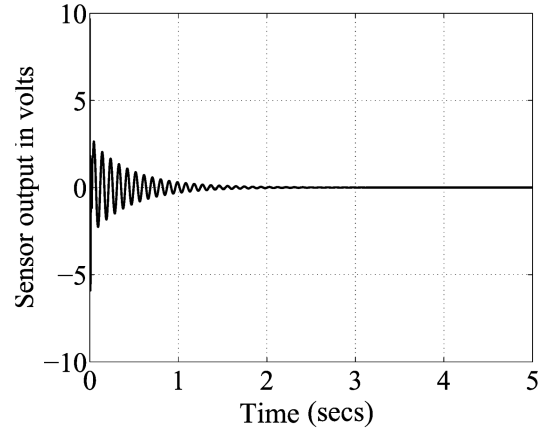


Fig. 9 Closed loop response of smart cantilever beam with aspect ratio=15

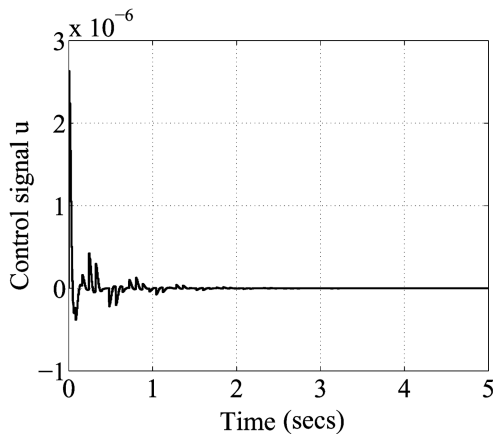


Fig. 10 Control signal of smart cantilever beam with aspect ratio=15

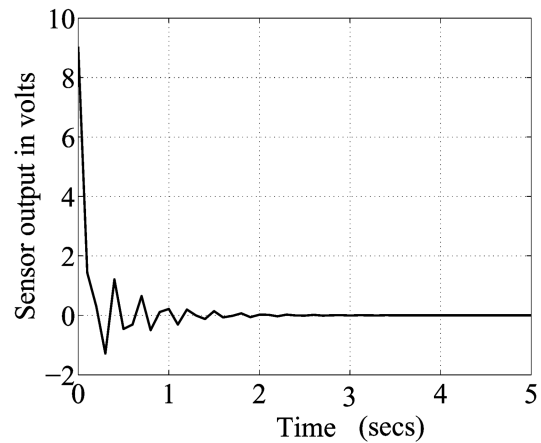


Fig. 11 Open loop response of smart cantilever beam with aspect ratio=10

0.5 mm by 2.4 cm. The first three natural frequencies calculated are 158.43 Hz, 932.41 Hz, and 1435.33 Hz respectively.

In the second case, the aspect ratio is taken equal to 10. The length of the beam element is 5 cm and its cross section is 5 mm by 2.4 cm. The length of the piezoelectric patch is 5 cm and its cross section is 0.5 mm by 2.4 cm. The first three natural frequencies calculated are 132.23 Hz, 792.38 Hz, and 1591.41 Hz respectively.

In the third case, the aspect ratio is taken equal to 8. The length of the beam element is 5 cm and its cross section is 6.25 mm by 2.4 cm. The length of the piezoelectric patch is 5 cm and its cross section is 0.5 mm by 2.4 cm. The first three natural frequencies calculated are 105.97 Hz, 644.1 Hz and 1495.83 Hz respectively.

A external force f_{ext} of 1 Newton is applied for duration of 50 ms at the free end of the beam for the 3 systems having different aspect ratios and the open loop responses of the system are obtained as shown in Figs. 8/11 and 14 respectively. Controllers based on the fast output sampling feedback control

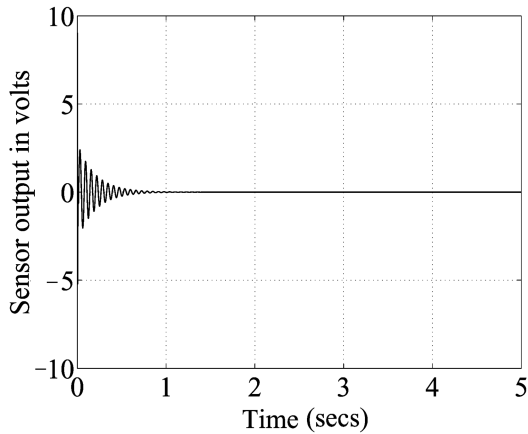


Fig. 12 Closed loop response of smart cantilever beam with aspect ratio=10

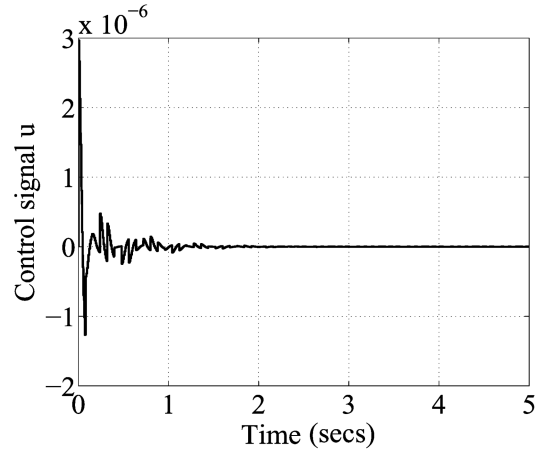


Fig. 13 Control signal of smart cantilever beam with aspect ratio=10

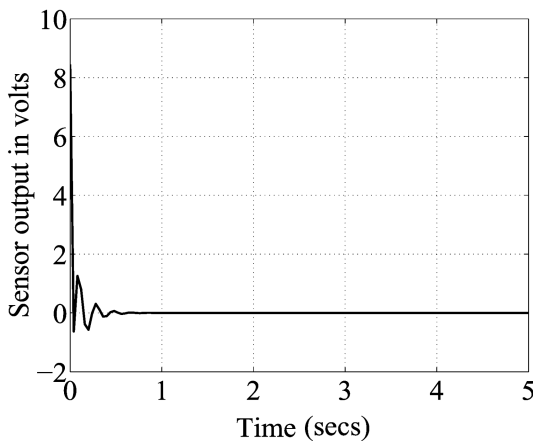


Fig. 14 Open loop response of smart cantilever beam with aspect ratio=8

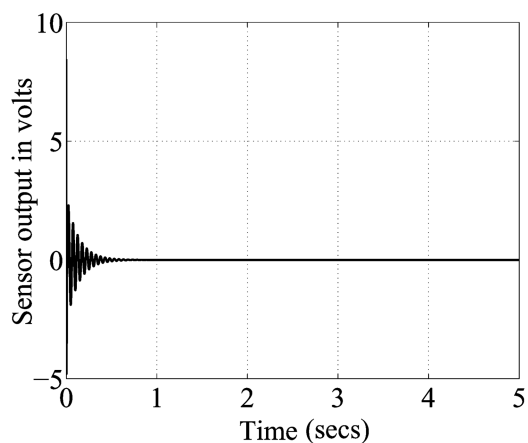


Fig. 15 Closed loop response of smart cantilever beam with aspect ratio=8

algorithm (Werner, *et al.* 1995) has been designed to control the first three modes of vibration of the smart cantilever beam for the 3 systems having different aspect ratios. The first task in designing the fast output sampling feedback controller is the selection of the sampling interval τ . The maximum bandwidth for the sensor/actuator locations on the beam are calculated (here, the third vibratory mode of the plant). Then, by using the existing empirical rules for selecting the sampling interval based on bandwidth, approximately 10 times of the maximum third vibration mode frequency of the system is selected. The sampling interval used is 0.07 sec. The sampling interval is divided into 10 subintervals ($N=10$).

The fast output sampling feedback gain matrix L for the system given in Eq. (59) is obtained by solving $LC \cong F$ using the LMI optimization method (Yong, Lam and Sun 1998). The closed loop impulse responses (sensor outputs y) with fast output sampling feedback gain L of the system shown in the Fig. 3 having different aspect ratios are shown in Figs. 9/12 and 15 respectively. The variation of the control signal u with time for the system shown in the Fig. 3 having different aspect ratios are shown in Figs. 10/13 and 16 respectively.

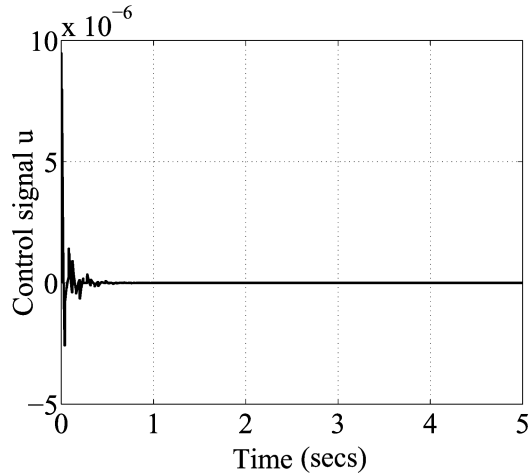


Fig. 16 Control signal of smart cantilever beam with aspect ratio=8

7. Conclusions

An integrated finite element model to analyze the vibration suppression capability of a smart cantilever beam with surface mounted piezoelectric devices based on Timoshenko beam theory is presented in this paper. Models are developed for various aspect ratios and their performance is compared with beam models based on Euler-Bernoulli beam theory for the same aspect ratios. It is shown that Timoshenko beam theory predicts a structure's response more accurately especially for higher modes of vibration for a wide range of aspect ratios. Different models of the smart cantilever beam have been obtained by varying the length to thickness (aspect) ratio of the beam from 8 to 15, the length of the beam is kept constant and the thickness of the beam is varied. 3 different cases have been considered (aspect ratio=8, 10 and 15) in our context. By comparing the open loop and closed loop responses, it is observed that

- In the first case for the aspect ratio=15, it was observed that there was an 89.4% decrease in settling time for the system after applying fast output sampling feedback control.
- Similarly, a change of 89.3% in settling time was observed for the case with aspect ratio=10 and
- A change of 89% in settling time was observed for the case with aspect ratio=8.

From the simulation results, it is observed that the first natural frequency predicted by both the theories is almost the same. Since many modes contribute to a structure's response, it can be inferred from the figures that there is a large difference in the second and third natural frequencies predicted by Timoshenko and Euler-Bernoulli beam theories especially for small length to thickness ratios (aspect ratio<10). Timoshenko beam theory can predict the dynamic characteristics of the beam more accurately over the entire range of length by thickness ratio. Since Timoshenko beam model is closer to the actual model it is used as the basis for controller design in our research work.

The limitations of Euler-Bernoulli beam theory such as the neglect of the shear have been considered here. In practical situations, a large number of modes of vibrations contribute to the structure's response. It has been shown that Euler-Bernoulli beam theory is not able to predict the transient response of a structure accurately, due to inability to predict higher natural frequencies accurately. Therefore, a controller based on Euler-Bernoulli beam theory will not perform satisfactorily

in controlling the higher modes of vibration of cantilever beam when the shear forces and the axial displacements are neglected. Timoshenko beam theory corrects the simplifying assumptions made in Euler-Bernoulli beam theory.

A fast output sampling feedback controller is designed for the Timoshenko beam model to suppress the vibration of the smart cantilever beam by considering the first three modes. It can be inferred from the simulation results that a fast output sampling feedback controller applied to a smart cantilever beam model based on Timoshenko beam theory is able to satisfactorily control higher modes of vibration of the smart cantilever beam for a wide range of aspect ratios. Also, the vibrations are damped out in a lesser time, which can be observed from the simulation results. Surface mounted piezoelectric sensors and actuators are usually placed at nearby the fixed end position of the structure to achieve most effective sensing and actuation. It can be inferred from the simulation results, that when the system is placed with this designed controller, the system's performance meets the design requirements. The designed FOS feedback controller requires constant gains and hence is easier to implement in real time.

References

- Aldraihem, O. J., Wetherhold, R. C. and Singh, T. (1997), "Distributed control of laminated beams: Timoshenko vs. Euler-Bernoulli Theory", *J. Intelligent Mater. Syst. and Struct.*, **8**, 149-157.
- Abramovich, H. (1998), "Deflection control of laminated composite beam with piezoceramic layers-closed form solution", *Compo. Struct.*, **43**(3), 217-131.
- Aldraihem, O. J. and Khdeir Ahmed, A. (2000), "Smart beams with extension and thickness-shear piezoelectric actuators", *Smart Mat. and Struct.*, **9**(1), 1-9.
- Ahmed, A. K. and Osama, J. A. (2001), "Deflection analysis of beams with extension and shear piezoelectric patches using discontinuity functions", *Smart Mater. and Struct.*, **10**(1), 212-220.
- Azulay, L. E. and Abramovich, H. (2004), "Piezoelectric actuation and sensing mechanisms - Closed form solutions", *Compo. Struct.*, **64**(3-4), 443-453.
- Baily, T. and Hubbard Jr., J. E. (1985), "Distributed piezoelectric polymer active vibration control of a cantilever beam", *J. Guidance, Control and Dyn.*, **8**(5), 605-611.
- Benjeddou, A., Trindade, M. A. and Ohayon, R. (1999), "New shear actuated smart structure beam finite element", *AIAA J.*, **37**, 378-383.
- Crawley, E. F. and De Luis, J. (1987), "Use of piezoelectric actuators as elements of intelligent structures", *AIAA J.*, **25**, 1373-1385.
- Chandrashekhara, K. and Varadarajan, S. (1997), "Adaptive shape control of composite beams with piezoelectric actuators", *J. Intelligent Mater. Sys. and Struct.*, **8**, 112-124.
- Culshaw, B. (1992), "Smart structure a concept or a reality", *J. of Systems and Control Eng.*, **26**(206), 1-8.
- Cooper, C. R. (1966), "Shear coefficient in Timoshenko beam theory", *ASME J. of Applied Mechanics*, **33**, 335-340.
- Choi, S. B., Cheong, C. and Kini, S. (1995), "Control of flexible structures by distributed piezo-film actuators and sensors", *J. Intelligent Mater. and Struct.*, **16**, 430-435.
- Doschner, C., and Enzmann, M. (1998), "On model based controller design for smart structure", *Smart Mechanical Systems Adaptronics SAE International USA*, 157-166.
- Donthireddy, P. and Chandrashekhara, K. (1996), "Modeling and shape control of composite beam with embedded piezoelectric actuators", *Compo. Struct.*, **35**(2), 237-244.
- Fanson, J. L. and Caughey, T. K. (1990), "Positive position feedback control for structures," *AIAA J.*, **18**(4), 717-723.
- Friedman, Z. and Kosmatka, J. B. (1993), "An improved two-node Timoshenko beam finite element", *Comput. and Struct.*, **47**(3), 473-481.
- Hanagud, S., Obal, M. W. and Callise, A. J. (1992), "Optimal vibration control by the use of piezoceramic sensors and actuators", *J. Guidance, Control and Dyn.*, **15**(5), 1199-1206.
- Hwang, W. and Park H. C. (1993), "Finite element modeling of piezoelectric sensors and actuators", *AIAA J.*

- 31(5), 930-937.
- Manjunath, T. C. and Bandyopadhyay, B (2004), "Vibration control of smart flexible cantilever beam using periodic output feedback", *Asian J. Control*, **6**, 74-87.
- Raja, S., Prathap, G. and Sinha, P. K. (2002), "Active vibration control of composite sandwich beams with piezoelectric extension-bending and shear actuators", *Smart Mater. and Struct.*, **11**(1), 63-71.
- Sun, C. T. and Zhang, X. D. (1995), "Use of thickness-shear mode in adaptive sandwich structures", *Smart Mater. and Struct.*, **4**(3), 202-206.
- Syrmos, V. L., Abdallah, P., Dorato, P. and Grigoriadis, K. (1997) "Static output feedback a survey", *Automatica*, **33**(2), 125-137.
- Thomas, J. and Abbas, B. A. H. (1975), "Finite element methods for dynamic analysis of timoshenko beam", *J. Sound Vib.*, **41**, 291-299.
- Umapathy, M. and Bandyopadhyay, B. (2000), "Vibration control of flexible beam through smart structure concept using periodic output feedback", *J. Sys. Sci.*, **26**(1), 23-46.
- Werner, H. and Furuta, K. (1995), "Simultaneous stabilization based on output measurements", *Kybernetika*, **31**(4), 395-411.
- Werner, H., (1998), "Multimodal robust control by fast output sampling - An LMI approach", *Automatica*, **34**(12), 1625-1630.
- Cao, Yong-Yan, Lam, J. and Sun, Y. X. (1998), "Static output feedback stabilization: An LMI approach", *Automatica*, **34**(12), 1641-1645.
- Zhang, X. D. and Sun, C. T. (1996), "Formulation of an adaptive sandwich beam", *Smart Mater. and Struct.*, **5**(6), 814-823.

Appendix

$[N_w]^T$, $[N_\theta]^T$, and $[N_a]^T$ are the mode shape functions (for displacement, rotation and acceleration) taking the shear ϕ into consideration and is obtained as (Friedman and Kosmatka 1993).

$$[N_w]^T = \begin{bmatrix} \frac{1}{(1+\phi)} \left\{ 2 \left(\frac{x}{L} \right)^3 - 3 \left(\frac{x}{L} \right)^2 - \phi \left(\frac{x}{L} \right) + (1+\phi) \right\} \\ \frac{L}{(1+\phi)} \left\{ \left(\frac{x}{L} \right)^3 - \left(2 + \frac{\phi}{2} \right) \left(\frac{x}{L} \right)^2 + \left(1 + \frac{\phi}{2} \right) \left(\frac{x}{L} \right) \right\} \\ - \frac{1}{(1+\phi)} \left\{ 2 \left(\frac{x}{L} \right)^3 - 3 \left(\frac{x}{L} \right)^2 - \phi \left(\frac{x}{L} \right) \right\} \\ \frac{L}{(1+\phi)} \left\{ \left(\frac{x}{L} \right)^3 - \left(1 - \frac{\phi}{2} \right) \left(\frac{x}{L} \right)^2 - \left(\frac{\phi}{2} \right) \left(\frac{x}{L} \right) \right\} \end{bmatrix}; \quad [N_\theta]^T = \begin{bmatrix} \frac{6}{(1+\phi)L} \left\{ \left(\frac{x}{L} \right)^2 - \left(\frac{x}{L} \right) \right\} \\ \frac{1}{(1+\phi)} \left\{ 3 \left(\frac{x}{L} \right)^2 - (4+\phi) \left(\frac{x}{L} \right) + (1+\phi) \right\} \\ - \frac{6}{(1+\phi)L} \left\{ \left(\frac{x}{L} \right)^2 - \left(\frac{x}{L} \right) \right\} \\ \frac{1}{(1+\phi)} \left\{ 3 \left(\frac{x}{L} \right)^2 - (2-\phi) \left(\frac{x}{L} \right) \right\} \end{bmatrix}$$

$$[N_a]^T = \begin{bmatrix} \frac{6}{(1+\phi)L} \left\{ \frac{2x}{L^2} - \frac{1}{L} \right\} \\ \frac{1}{(1+\phi)L} \left\{ \frac{6x}{L} - (4+\phi) \right\} \\ - \frac{6}{(1+\phi)L} \left\{ \frac{6x}{L^2} - \frac{1}{L} \right\} \\ \frac{1}{(1+\phi)} \left\{ \frac{6x}{L^2} - \left(\frac{2-\phi}{L} \right) \right\} \end{bmatrix}$$

where L is the length of beam element and ϕ is the ratio of the beam bending stiffness to shear stiffness and is given by

$$\phi = \frac{12}{L^2} \left(\frac{EI}{KGA} \right)$$

Translational inertia matrix $[M_{\rho A}]$ and rotational inertia matrix $[M_{\rho I}]$ with the shear is obtained as

$$[M_{\rho A}] = \frac{\rho I}{210(1+\phi)^2} \begin{bmatrix} (70\phi^2 + 147\phi + 78) & (35\phi^2 + 77\phi + 44)\frac{L}{4} & (35\phi^2 + 63\phi + 27) & -(35\phi^2 + 63\phi + 26)\frac{L}{4} \\ (35\phi^2 + 77\phi + 44)\frac{L}{4} & (7\phi^2 + 14\phi + 8)\frac{L^2}{4} & (35\phi^2 + 63\phi + 26)\frac{L}{4} & -(7\phi^2 + 14\phi + 6)\frac{L^2}{4} \\ (35\phi^2 + 63\phi + 27) & (35\phi^2 + 63\phi + 26)\frac{L}{4} & (70\phi^2 + 147\phi + 78) & -(35\phi^2 + 77\phi + 44)\frac{L}{4} \\ -(35\phi^2 + 63\phi + 26)\frac{L}{4} & -(7\phi^2 + 14\phi + 6)\frac{L^2}{4} & -(35\phi^2 + 77\phi + 44)\frac{L}{4} & (7\phi^2 + 14\phi + 8)\frac{L^2}{4} \end{bmatrix}$$

$$[M_{\rho I}] = \begin{bmatrix} 36 & -(15\phi - 3)L & -36 & -(15\phi - 3)L \\ -(15\phi - 3)L & (10\phi^2 + 5\phi + 4)L^2 & (15\phi - 3)L & (5\phi^2 - 5\phi - 1)L^2 \\ (10\phi^2 + 5\phi + 4)L^2 & (15\phi - 3)L & 36 & (15\phi - 3)L \\ -(15\phi - 3)L & (5\phi^2 - 5\phi - 1)L^2 & (15\phi - 3)L & (10\phi^2 + 5\phi + 4)L^2 \end{bmatrix}$$

The stiffness matrix $[K_b]$ of the beam element with the shear is given by

$$[K^b] = \frac{EI}{(1+\phi)L^3} \begin{bmatrix} 12 & 6L & -12 & 6L \\ 6L & (4+\phi)L^2 & -6L & (2-\phi)L^2 \\ -12 & -6L & 12 & -6L \\ 6L & (2-\phi)L^2 & -6L & (4+\phi)L^2 \end{bmatrix}$$

When ϕ is neglected, the mass matrix and the stiffness matrix reduces to

$$[M_{\rho A}] = \frac{\rho I}{210} \begin{bmatrix} 78 & 11L & 27 & -13\frac{L}{2} \\ 11L & 2L^2 & 13\frac{L}{2} & -3\frac{L^2}{2} \\ 27 & 13\frac{L}{2} & 78 & -11L \\ -13\frac{L}{2} & -3\frac{L^2}{2} & -11L & 2L^2 \end{bmatrix} = \frac{\rho I}{420} \begin{bmatrix} 156 & 22L & 54 & -13L \\ 22L & 4L^2 & 13L & -3L^2 \\ 54 & 13L & 156 & -22L \\ -13L & -3L^2 & -22L & 4L^2 \end{bmatrix}$$

$$[K] = \frac{EI}{L^3} \begin{bmatrix} 12 & 6L & -12 & 6L \\ 6L & 4L^2 & -6L & 2L^2 \\ -12 & -6L & 12 & -6L \\ 6L & 2L^2 & -6L & 4L^2 \end{bmatrix}$$

Notation

FOS	Fast Output Sampling
SISO	Single Input Single Output
MIMO	Multi Input Multi Output
FEM	Finite Element Method
FE	Finite Element
LMI	Linear Matrix Inequalities
MR	Magneto Rheological
ER	Electro Rheological
PVDF	Poly Vinylidene Flouride
CF	Clamped Free
CC	Clamped Clamped
CT	Continuous Time
DT	Discrete Time
HOBT	Higher Order Beam Theory
RHS	Right Hand Side
LTI	Linear Time Invariant
EB	Euler-Bernoulli
PZT	Lead Zirconate Titanate
<i>FC</i>	